

Development, experimental validation and sensitivity analysis of a mathematical model of biofiltration for hydrogen sulfide removal

Pairote Satiracoo, Prayad Pokethitiyook, Yongwimon Lenbury,
Siraporn Potivichayanon, Ravi P. Agarwal

Abstract—A dynamic model which describes the removal of hydrogen sulfide from contaminated air in a biotrickling filter has been developed. The model includes mathematical expressions for contaminant mass transfer and biodegradation kinetics. According to the experimental results which reveal the influence of biofilm thickness on the hydrogen removal efficiency of the biotrickling filter, the proposed model attempts to describe the loss of biomass and changes in biofilm thickness. The loss of biofilm due to shear or sloughing is also explicitly incorporated into the model. Model evaluation is performed by comparison of model simulations with experimental data. When the model are simulated under the assumption of unrestricted growth of microorganisms, the model can predict the behavior of the system under various operating conditions. When including biofilm detachment, the model simulations show improvement in prediction of both the removal efficiency and biofilm thickness in comparison to the model simulations under the unrestricted growth condition. Furthermore, a sensitivity analysis of model parameters shows that the gas and liquid flow rates have a significant effect on hydrogen sulfide removal, while the maximum growth rate and biomass yield have an intermediate influence.

Keywords—Biofilm, biofilm thickness, biotrickling filter, mathematical model.

P. Satiracoo is with Department of Mathematics, Faculty of Science, Mahidol University, Bangkok 10400, Thailand and the Centre of Excellence in Mathematics, CHE, 328 Si Ayutthaya Road, Bangkok 10400, Thailand (corresponding author; phone +662-201-5345; fax 662-201-5345; email: pairote.sat@mahidol.ac.th).

P. Pokethitiyook is with Department of Biology, Faculty of Science, Mahidol University, Bangkok 10400, Thailand (email: prayad.pok@mahidol.ac.th).

Y. Lenbury is with Department of Mathematics, Faculty of Science, Mahidol University, Bangkok 10400, Thailand and the Centre of Excellence in Mathematics, CHE, 328 Si Ayutthaya Road, Bangkok 10400, Thailand (email: yongwimon.len@mahidol.ac.th).

Siraporn Potivichayanon is with School of Environmental Health, Institute of Medicine, Suranaree University of Technology, Nakhon Ratchasima, 30000 Thailand (e-mail: siraporn@sut.ac.th).

Ravi P. Agarwal is with Department of Mathematics, Texas A&M University-Kingsville, TX 78363 USA (e-mail: agarwal@tamuk.edu).

I. INTRODUCTION

Hydrogen sulfide is a highly toxic compound which can be produced from biological waste treatment and some industrial processes including food processing, iron and steel manufacturing [1], and petroleum refinery [2]. It is a colorless, flammable gas that can be detected at relatively low concentrations. At concentrations above 10 ppm, it can affect human health [3]. It is also highly corrosive, which can result in costly damage to equipment and piping systems used in gas handling.

One of the most effective methods for hydrogen sulfide removal is biological treatment because the process requires no chemical addition and offers lower operating cost. In biotrickling filters, contaminated gas flows through a packed column. The packing is made of an inert material, such as plastics, glasses or ceramics which provides support to microorganisms. After gas absorption through the biofilm, biological degradation of contaminated gas is performed. Microorganisms use the pollutant as a source of energy and cleaned air is the required final product. In order to achieve complete degradation, a liquid needs to be transferred to the packed column. The liquid can also be used to maintain the temperature, pH, and nutrient level in the biotrickling filter.

Recently, several mathematical models have been proposed to describe the elimination of volatile organic compounds in biotrickling filters [4], [5]. Only a few models are specifically applied to the treatment of hydrogen sulfide and other odorous gases. Kim and Deshusses [6] proposed a new dynamic model to simulate the basic transport and biological processes of hydrogen sulfide reduction in the biotrickling filter. The model considers the effect of the gas-biofilm mass transport resistance, but assumes constant biofilm thickness. Li *et al.* [7] developed a biotrickling filter model for the degradation of hydrogen sulfide that included the biomass accumulation within the biofilm. A Monod kinetic expression was assumed for biomass growth as a function of existing concentration of biomass and the

concentration of contaminant. In this model, the biofilm consists of active and inactive biomass. The active biomass is responsible for substrate removal, while inactive biomass plays no role in substrate removal. However, a constant biofilm thickness is assumed.

Nevertheless, the existing models do not sufficiently take into consideration the fact that the biofilm thickness also influences the removal efficiency. The experimental results from [8] reveal that there is a substantial drop in removal efficiency when a loss of biomass occurs during the experiment. Therefore, the main objective of this work is to develop a mathematical model that would adequately describe the dynamics of the biotrickling filter for the treatment of odorous waste gas. The study focuses on the effect of the biofilm development on the purification efficiency. Main factors including shear stress and biomass sloughing that control the growth of the biomass are taken into account. Furthermore, the model is validated using experimental results and model simulations are performed to study sensitivity analysis to selected parameters.

II. MATERIALS AND METHODS

A. Formulation of mathematical model

Biotrickling filter model involves several complex phenomena including mass transport by advective flow, absorption, diffusion, and biodegradation. To formulate the mathematical model, substrate degradation and variation of the biofilm thickness are modeled by using the approach in [9]. In addition, mass transport in the gas and liquid phases and mass transfer at the interfaces are based on conservative principles of mass, which are similar to previous works ([6], [7]).

1) Mass balance of the contaminant in the gas and liquid phases

Model equations are based on the following typical assumptions. Contaminant concentrations in the gas and liquid phases are assumed to be uniform across the biotrickling filter cross section. Therefore a plug flow pattern is considered for gas and liquid flow. Gas-liquid and liquid-biofilm interfaces are at equilibrium, which can be described by Henry's law. There is no contaminant degradation in the gas and liquid phases. The mass balance equations that describe the axial gas and liquid concentration profiles of the contaminant are

$$\begin{aligned} V_g \frac{\partial C_g(t, \bar{z})}{\partial t} &= -Q_g \frac{\partial C_g}{\partial \bar{z}} - K_g A_d \left(\frac{C_g}{H} - C_\ell \right) \\ V_\ell \frac{\partial C_\ell(t, \bar{z})}{\partial t} &= Q_\ell \frac{\partial C_\ell}{\partial \bar{z}} + K_g A_d \left(\frac{C_g}{H} - C_\ell \right) \\ &\quad - K_\ell A_d (C_\ell - C_b(t, \bar{z}, L)) \end{aligned} \quad (1)$$

where C_g, C_ℓ are the concentrations of contaminant in gas and liquid phases, Q_g, Q_ℓ are volumetric gas and liquid flow rates, V_g, V_ℓ are the volumes of gas and liquid phases, A_d is diffusion surface area, K_g, K_ℓ are the gas-liquid and liquid-biofilm mass transfer coefficients and \bar{z} is the dimensionless axial coordinate. The initial and boundary conditions are given by

$$\begin{aligned} C_g(0, \bar{z}) &= 0, & C_g(t, 0) &= C_{g,in}, \\ C_\ell(0, \bar{z}) &= 0, & C_\ell(t, 1) &= 0. \end{aligned}$$

2) Mass balance of the contaminant in the biofilm phase

In the biofilm, the only mass transport mechanism is the diffusion governed by Fick's law. Biological reaction is described by the Monod equation for which hydrogen sulfide is the only growth limiting substrate. Assuming that the biofilm growth occurs in the direction normal to liquid-film interface, the variation of biomass and substrate will only be considered in this direction. The mass balance equation of transversal concentrations of the contaminant in the biofilm phase is

$$\frac{\partial C_b(t, \bar{z}, x)}{\partial t} = r + \frac{\partial}{\partial x} \left(D \frac{\partial C_b}{\partial x} \right), \quad (2)$$

where C_b is the concentration of contaminant in biofilm phases, D is the contaminant diffusion coefficient and x is the biofilm depth coordinate. The boundary conditions are given by

$$\begin{aligned} \frac{\partial C_b}{\partial x}(t, \bar{z}, 0) &= 0 \\ D \frac{\partial C_b}{\partial x}(t, \bar{z}, L) &= K_\ell (C_\ell - C_b(t, \bar{z}, L)). \end{aligned}$$

The substrate consumption rate r in (2) is given by

$$r = -\rho m_{\max} \mu_{\max} \frac{1}{Y} \frac{C_b}{C_b + K_s}$$

where ρ is biofilm density, μ_{\max} is the maximum growth rate of biomass, Y is the biomass yield coefficient and K_s is the Monod half saturation constant.

3) Biofilm development

The biofilm consists of active biomass that is responsible for contaminant degradation and inactive biomass that plays no role in contaminant removal. The variables m_{act}, m_{inert} are the local volume fraction of active and inactive biomass respectively ($m_{act} + m_{inert}$). Transport of biomass is governed by an advective process with the rate of biofilm expansion u . Based on a conservation law [9], the mass balance equations for biomass accumulation and its boundary conditions are described by

$$\frac{\partial m_{\text{act}}}{\partial t} = (\mu_{\text{act}} - \bar{\mu})m_{\text{act}} - u \frac{\partial m_{\text{act}}}{\partial x}, \quad (3)$$

$$\frac{\partial m_{\text{act}}}{\partial x}(t, 0) = 0,$$

where the specific growth rate of the active and inactive biomass can be obtained from

$$\mu_{\text{act}} = \mu_{\text{max}} \frac{C_b}{C_b + K_s} - d_k, \quad \mu_{\text{inert}} = d_k \frac{m_{\text{act}}}{m_{\text{inert}}}.$$

The rate of biofilm expansion is defined by

$$u(t, x) = \int_0^x \bar{\mu}(t, x') dx',$$

which is the integral of average local growth rate $\bar{\mu}(t, x) = \mu_{\text{act}}m_{\text{act}} + \mu_{\text{inert}}m_{\text{inert}}$ over the entire length of the biofilm.

The variation in biofilm thickness with time can be expressed as

$$\frac{dL}{dt} = u(t, L) + \sigma(t), \quad (4)$$

where $\sigma(t)$ is the detachment rate of biofilm.

B. Biotrickling filter

A schematic diagram of the biotrickling filter is shown in Fig.1. The biotrickling filter is a glass column of 0.03 m in diameter and 0.5 m in height. The column is packed with polypropylene pall rings to the working height of 0.15 m. Before filling in the column with the packing materials, the immobilization process of bacterial cells is initiated by transferring the packing materials into thiosulfate broth containing the microorganisms. Thus, the packing materials has an active biofilm of hydrogen sulfide oxidizing bacteria for starting up the biotrickling filter experiments. The biotrickling filter is operated with gas flowing upward and recycled liquid nutrient medium flowing downward. The energy source for microorganism growth is derived from the hydrogen sulfide oxidation in the biotrickling filter column. All experiments have been operated in continuous mode at room temperature. The temperatures of all experiments were in the range of 28.3-33.0°C, which did not affect removal efficiency. In addition, the pH values in the recirculation tank slightly decreased in all experiments from 6.9 to 6.5.

C. Numerical solution

The set of partial differential equations from the mass balance of biotrickling filter has been solved by discretization in space. The resulting set of equations has been solved in MATLAB. To simplify the numerical simulations, quasi-steady state concentration profiles in the biofilm are assumed ([4], [5]). This means that the time variation of the biofilm thickness is slower than the variation of the contaminant concentration. Therefore, axial concentrations of

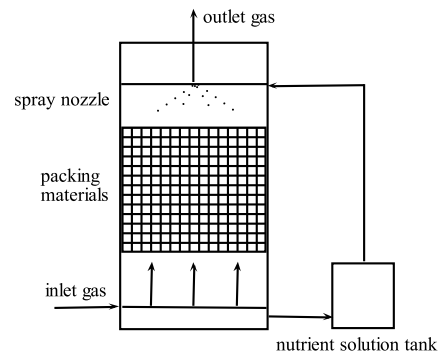


Fig. 1 A schematic diagram of the biotrickling filter.

contaminant have been calculated assuming a fixed biofilm thickness while the calculation of transversal biofilm concentration profiles has been obtained assuming steady-state concentration profiles.

D. Parameters for model prediction

For parameter estimation and data fitting, differential evolution (DE) algorithm developed in [10] is employed. The differential evolution which is a stochastic search algorithm has been successfully used to solve various optimization problems ([11], [12]). The optimal estimate of the parameters is obtained by minimizing the objective function of the form:

$$\left[\frac{1}{n-1} \sum_{i=1}^n \left(\frac{C_{\text{g,out}}(t_i) - \hat{C}_{\text{g,out}}(t_i)}{C_{\text{g,out}}(t_i)} \right)^2 \right]^{\frac{1}{2}} \quad (5)$$

where $C_{\text{g,out}}(t_i)$, $\hat{C}_{\text{g,out}}(t_i)$ are measured effluent concentration and model output effluent concentration respectively, and n is the number of measured data points. Model parameters can be classified into following main groups: kinetic, physical parameters and system specification.

1) Kinetic and stoichiometric parameters

Microorganisms, *Alcaligenes faecalis* MU2_03 were isolated from an aeration tank at Si-Phraya municipal wastewater treatment plant in Bangkok. The bacteria are reported in [13] as microorganisms capable for the removal of hydrogen sulfide. A thiosulfate broth composition was the medium used for bacteria culture. After the isolation of microorganisms, their growth was studied by the colony count technique. The bacterial numbers are determined as colony forming unit per ml (CFU/ml). During the growth studies, pH remained within ± 0.1 and could be considered a negligible change. The values of the kinetic parameters including the maximum growth rate μ_{max} , the substrate saturation constant K_s and biomass yield Y are determined from this suspended culture. Therefore, the kinetic parameters of biomass immobilized on the packing surface are

assumed to be the same as those of the culture when it is suspended in growth medium. The parameters are obtained by fitting the data to the solution of the well-known differential system:

$$\frac{dN}{dt} = \frac{\mu_{\max} CN}{K_s + C} \quad (6)$$

$$\frac{dC}{dt} = -\frac{\mu_{\max} CN}{Y(K_s + C)}, \quad (7)$$

where N and C represent the bacterial number and the nutrient concentration respectively. The parameter values are presented in Table 1. Comparison of the model prediction and experimental data for the bacterial growth is shown in Figure 2. The model simulation agrees reasonably well with the experimental data.

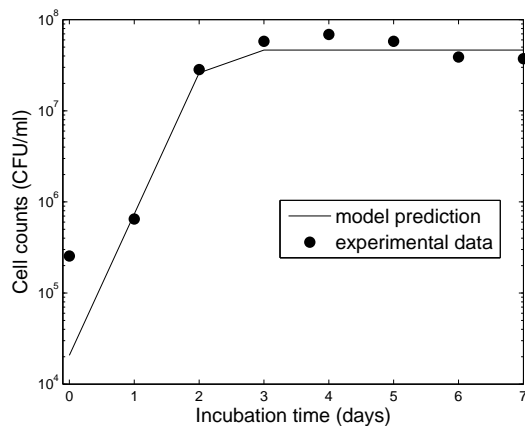


Fig. 2 The growth curve of MU2.03, together with the corresponding model simulation.

Table 1 Kinetic parameters values for solving model equations

Parameter	Value	Unit
μ_{\max}	3.57	1/day
K_s	3.44×10^{-4}	g/m ³
Y	0.05	—
d_k	0.78	1/day
ρ	1818.28	g/m ³

In addition to the three preceding kinetic parameters, the values of biofilm density ρ and decay rate coefficient d_k are determined by fitting data from the experiment 5 (details in section III.) of the biotrickling filter to the solution of the model equations.

2) Physical parameters

The diffusion area of active biomass is determined from the following equation [14]

$$\frac{A_d}{A_t} = 1 - \exp \left[-1.45 \left(\frac{\sigma_p}{\sigma_\ell} \right)^{0.75} \left(\frac{Q_\ell \rho_\ell}{SA_t \mu_\ell} \right)^{0.1} \times \left(\left(\frac{Q_\ell \rho_\ell}{S} \right)^2 \frac{A_t}{\rho_\ell^2 g} \right)^{-0.05} \left(\left(\frac{Q_\ell \rho_\ell}{S} \right)^2 \frac{1}{\rho_\ell \sigma_\ell A_t} \right)^{0.2} \right]. \quad (8)$$

It should be emphasized that the diffusion area of active biomass changes as the liquid flow rate is varied.

The gas and liquid mass transfer coefficients are determined from the following equations

$$\frac{\xi_1 K_g}{A_t D_g} = 5.23 \left(\frac{Q_g \rho_g}{SA_d \mu_g} \right)^{0.7} \left(\frac{\mu_g}{\rho_g D_g} \right)^{1/3} (A_t d_p)^{-2} \quad (9)$$

$$\xi_2 K_\ell \left(\frac{\rho_\ell}{\mu_\ell g} \right)^{1/3} = 0.0051 \left(\frac{Q_\ell \rho_\ell}{SA_d \mu_g} \right)^{2/3} \left(\frac{\mu_\ell}{\rho_\ell D_\ell} \right)^{-0.5} \times (A_t d_p)^{-0.4}. \quad (10)$$

The correction factors ξ_1 and ξ_2 in (9) and (10) have been used in previous studies [14]. In the present study, the values of the correction factors determined by fitting the experimental data of the biotrickling filter with the solutions of the model equations are set as follows: $\xi_1 = 2.09$ and $\xi_2 = 0.05$ at a liquid flow rate of 13 ml/min and $\xi_1 = 0.54$ and $\xi_2 = 0.89$ at a liquid flow rate of 35 ml/min. The other physical parameters and numerical coefficients appeared in (8), (9), and (10) have been taken from the literature and the experimental data, which are shown in Table 2.

III. RESULTS AND DISCUSSION

In order to verify the proposed model, model evaluation has been performed by comparing model predictions with experimental data obtained from [8] and [13]. Subsequently, detachment from biofilm possibly caused by sloughing or shear stress is taken into account for the study of the biofilm growth and its effect on the removal efficiency of the biotrickling filter.

A. Comparison between experimental results and model predictions

The experiments were operated for 6 hours under various operating conditions [13]. The packed column was set at 15 cm. Due to the lack of information in biofilm growth, the loss of the biofilm due to sloughing and shearing is neglected. Therefore, the detachment rate of biofilm σ in (4) is assumed to be 0.

Table 2 Physical parameters values from [14], [15] and system specification for solving model equations

Parameter	Symbol	Value	Unit
diffusion of hydrogen sulfide in air	D_g	2.7×10^{-5}	m^2/s
diffusion of hydrogen sulfide in water	D_ℓ	1.61×10^{-9}	m^2/s
gas viscosity	μ_g	0.018×10^{-3}	$\text{kg}/(\text{m}\cdot\text{s})$
gas density	ρ_g	1.193	kg/m^3
liquid viscosity	μ_ℓ	0.982×10^{-3}	$\text{kg}/(\text{m}\cdot\text{s})$
liquid density	ρ_ℓ	997.85	kg/m^3
surface tension of liquid	σ_ℓ	72×10^{-3}	N/m
cross sectional area of packed column	S	7.07×10^{-4}	m^2
specific surface area of packing material	A_t	206.81	$1/\text{m}$
packing diameter	d_p	0.025	m
surface tension of packing material	σ_p	0.033	N/m

The results of the experiments 1-6 and the model predictions are shown in Fig.3. The average values of removal efficiencies obtained in each experiment are plotted against various inlet gas concentrations at a fixed gas flow rate of 500 ml/min and liquid flow rates of 13 and 35 ml/min, respectively. The removal efficiency is obtained from the following expression:

$$\text{Removal efficiency}(\%) = \frac{C_{g,\text{in}} - C_{g,\text{out}}}{C_{g,\text{in}}} \times 100.$$

It can be seen that the model is able to predict qualitatively and quantitatively the behavior of the system under the operation conditions. The removal efficiency decreases with the increase of inlet gas concentration. This is consistent with the experiments performed earlier in [16]. In addition, the similar varying tendency of removal efficiency with the inlet gas concentration can be observed from the experiment results and the model predictions. In Fig.3(b), the model underestimates the removal efficiency in experiments 2 and 4. The values between the model predictions and the experimental results differ by 7% and 3% at 10 ppm and 20 ppm of inlet gas concentration respectively. However, these correspond to only 0.7 ppm and 0.6 ppm differences in outlet gas concentrations.

Experiment evolution for outlet hydrogen sulfide concentrations and numerical solutions in the experiments 1, 2, 7, and 8 are presented in Fig.4. The inlet gas concentrations used in experiments 1 and 2 were set at 10 ppm, while the higher inlet gas concentration of 80 ppm were operated in experiments 7 and 8. It can be demonstrated that the predicted outlet concentrations for both low and high inlet gas concentrations are in good agreement with the experimental results.

When the gas flow rate was decreased from 500 ml/min (experiments 5 and 6 with inlet gas concentration of 40 ppm) to 375 ml/min (experiments 7 and 8 with inlet gas concentration of 80 ppm) the removal efficiency increased to over 70%. In addition, if the gas flow rate was reduced to 200 ml/min in experiments 9 and 10 and the inlet gas concentration were set at 100 ppm, the removal efficiency

increased to over 85%. The experimental and simulated removal efficiencies plotted as a function of the gas flow rate (Fig.5) show that the model is capable of accurately predicting the behavior of the biotrickling filter.

B. Effect of the biofilm thickness on the removal efficiency

The growth of biofilm and its effect on the removal efficiency have been investigated by simulating the proposed mathematical model. The model predictions are compared with the experimental data given by [8]. The operating parameters were set with the inlet gas concentration of 20 ppm, the gas and liquid flow rates of 250 ml/min and 13 ml/min, respectively and the height of packing materials of 30 cm. The experiment was run for 15 days. During this period, the biofilm thickness of the packing materials at the middle of the biotrickling filter column was measured using the confocal laser scanning microscope. Figure 6 shows the removal efficiency and the development of biofilm with time between the experimental results and the model predictions. The experimental results reveals that the removal efficiency increases when the biofilm thickness increases. The approximation for the initial thickness is 25 μm . Then, the biofilm thickness is lowered to about 21 μm on day 2. This may be due to the dying or sloughing of the biofilm. However, it regrew rapidly with an increase in thickness of 37.5 μm on day 3 and the optimal removal efficiency of 95% was achieved. Subsequently, the removal efficiency decreased to 90% which was possibly due to a decrease in the biofilm thickness on day 5. When the biofilm thickness reached the highest peaks again on day 9 and 11, the biotrickling filter achieved the highest removal efficiency of 95%. However, the lower removal efficiencies were observed on day 13 when the biofilm thickness substantially decreased.

The model was first simulated under the unrestricted growth condition, i.e. the detachment rate of biofilm $\sigma = 0$ was assumed. For parameter estimation and data fitting with the measured biofilm thickness, the modified objec-

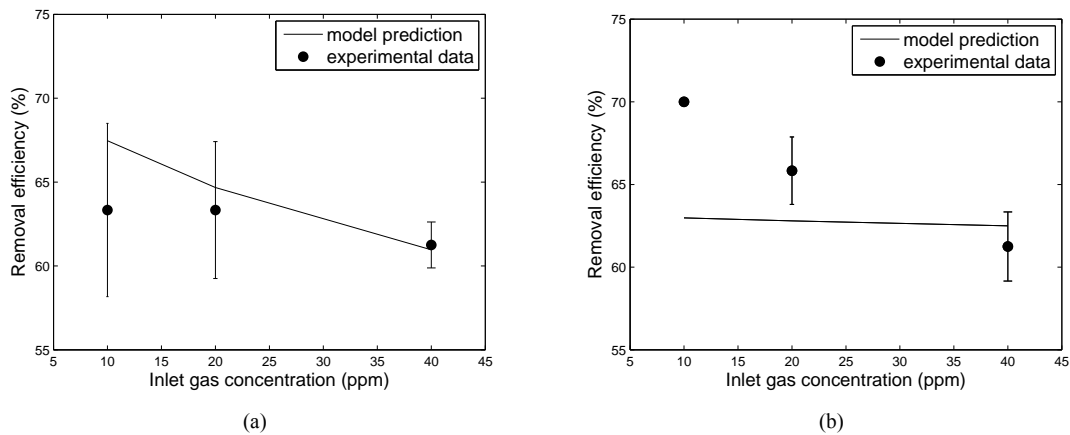


Fig. 3 Comparison of removal efficiencies between experimental data and numerical simulations (a) in the experiments 1, 3, and 5 with the gas flow rate of 500 ml/min and the liquid flow rates of 13 ml/min and (b) in the experiments 2, 4, and 6 with the gas flow rate of 500 ml/min and the liquid flow rates of 35 ml/min.

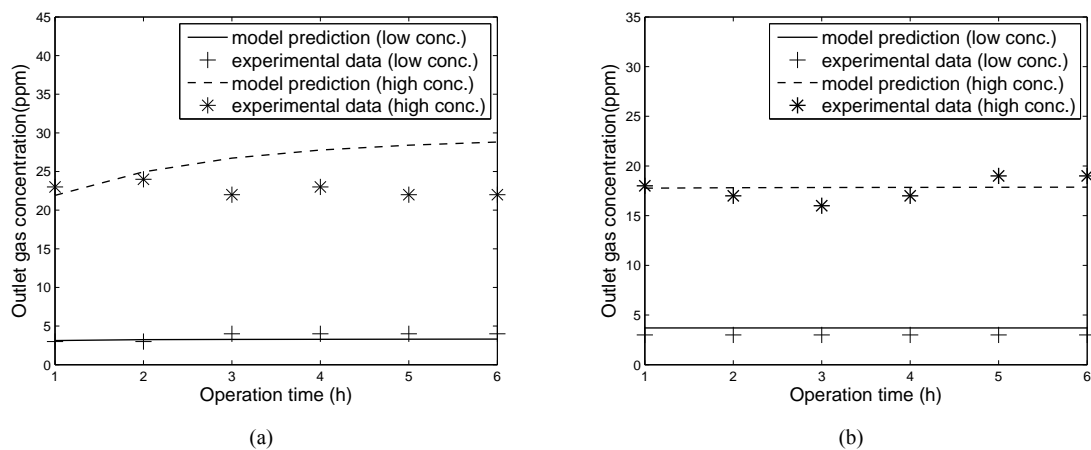


Fig. 4 Experiment evolution for outlet hydrogen sulfide concentrations and numerical solutions (a) in the experiments 1 and 7 and (b) in the experiments 2 and 8.

tive function was defined as the sum of the expression in (5) for the effluent gas concentrations and the analogous expression for the biofilm thickness. The minimum objective function of 0.912 was obtained. The model prediction shows that the removal efficiency slowly decreases from 94.6 to 93.5 on day 11 and then increases to 93.7 on day 15, while the biofilm thickness increases exponentially during the first nine days and then continues to increase with a constant rate throughout the remaining period.

Fluctuations of the biofilm are usually spontaneous, which can be observed in Fig. 6. Very little is known about the biological, chemical, and physical mechanisms of detachment [17]. In this study, biofilm detachment probably caused by shear stress or sloughing have been included in the model simulation. The detachment rate σ of biofilm in

(4) is defined as

$$\sigma(t) = c(L(t) - L_b)$$

where c is the detachment coefficient, L_b is the base biofilm thickness. The dynamics of biofilm detachment from the experiments yield on the average one detachment event every 3 days. In the simulation, $L_b = 30\mu\text{m}$ was assumed during detachment events except only the first period of detachment where $L_b = 21\mu\text{m}$ was used instead. The detachment coefficient c is given by

$$c = \begin{cases} 0, & \text{without detachment} \\ \text{constant}, & \text{during detachment event} \end{cases}$$

The duration of each biofilm detachment was assumed to be 0.5 day. The minimum modified objective function of

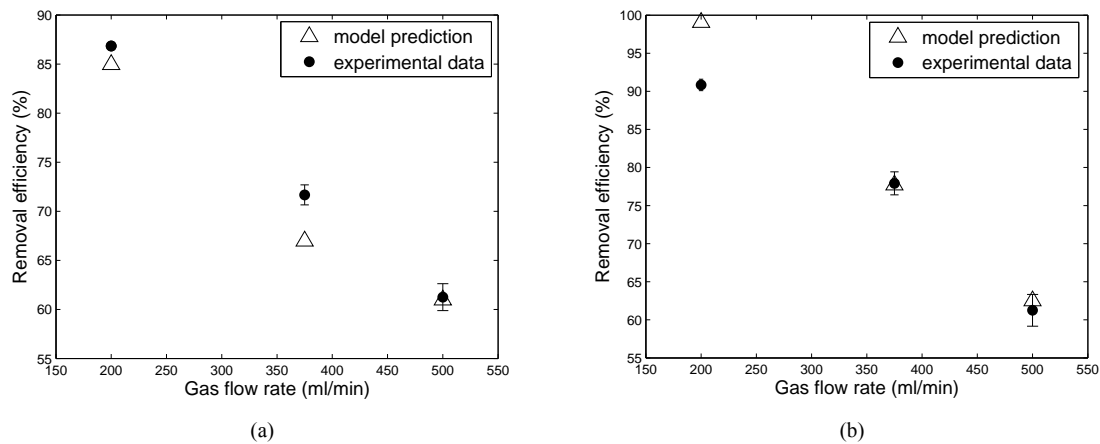


Fig. 5 Comparison of removal efficiencies between experimental data and numerical simulations (a) in the experiments 5, 7, and 9 with the inlet gas concentration of 40, 80, and 100 respectively and the liquid flow rates of 13 ml/min and (b) in the experiments 6, 8, and 10 with the inlet gas concentration of 40, 80, and 100 respectively and the liquid flow rates of 35 ml/min.

0.561 was achieved with the detachment coefficient $c = 3.1, 0.1, 7.9, 0.6,$ and $5.5 d^{-1}$ for the first up to the fifth detachment events respectively. The model simulation shows improvement in prediction both in the removal efficiency and the biofilm thickness as compared to the model prediction under the unrestricted growth condition. In particular, the model prediction is in good agreement with the measured biofilm thickness. Furthermore, the simulated biofilm thickness and the removal efficiency significantly drop and the biofilm thickness agrees with the mean of the measured biofilm thickness on day 13. The model under this dynamics condition is able to predict qualitatively the behaviour of the biotrickling filter.

C. Sensitivity analysis of model parameters

A sensitivity analysis has been performed for gas and liquid flow rates (Q_g, Q_ℓ), kinetic, and stoichiometric parameters (μ_{\max}, K_s, Y, d_k). Model simulations were run until a steady state of outlet concentration was achieved under the same operating conditions as in the previous section. The detachment rate of biofilm σ was also set to 0. The sensitivity analysis was carried out by increasing and decreasing 10% the values of the parameters and comparing the relative change of the outlet concentrations and the removal efficiencies to a relative change of the value of the parameter by the following expression [18]:

$$\text{Sensitivity} = \frac{\Delta V/V_d}{|\Delta P/P_d|},$$

where ΔV means the difference between the simulated variable under the new conditions and the value of the variable in the default conditions (V_d). Similarly, ΔP means the difference between the value of the parameter at the $\pm 10\%$ change and the value of the default parameter (P_d).

Under the operating conditions in this study, the gas and liquid flow rates have a significant effect on the removal efficiency. The removal efficiency is more sensitive to the gas velocity than the liquid velocity. This is possibly due to lesser substrate entering the biotrickling filter when the gas flow rate is reduced. All other parameters have a minor influence on the performance of the biotrickling filter. Therefore, a decrease in the gas flow rate and an increase in the liquid flow rate result in an improvement on the performance of the biotrickling filter.

Table 3 Sensitivity analysis for outlet concentration and removal efficiency

Parameter	$\Delta(\%)$	Sensitivity, $C_{g,out}$	Sensitivity, RE
Q_g	+10	1.51	-0.09
	-10	-1.48	0.09
Q_ℓ	+10	-0.89	0.05
	-10	1.09	-0.07
μ_{\max}	+10	-0.04	0.003
	-10	0.05	-0.003
K_s	+10	0.03	-0.002
	-10	-0.03	0.002
Y	+10	0.003	-0.000
	-10	-0.003	0.000
d_k	+10	0.03	-0.002
	-10	-0.03	0.002

IV. CONCLUSIONS

A new mathematical model has been developed to describe the dynamics in the biotrickling filter. The fundamental assumptions for this model are a combination of the

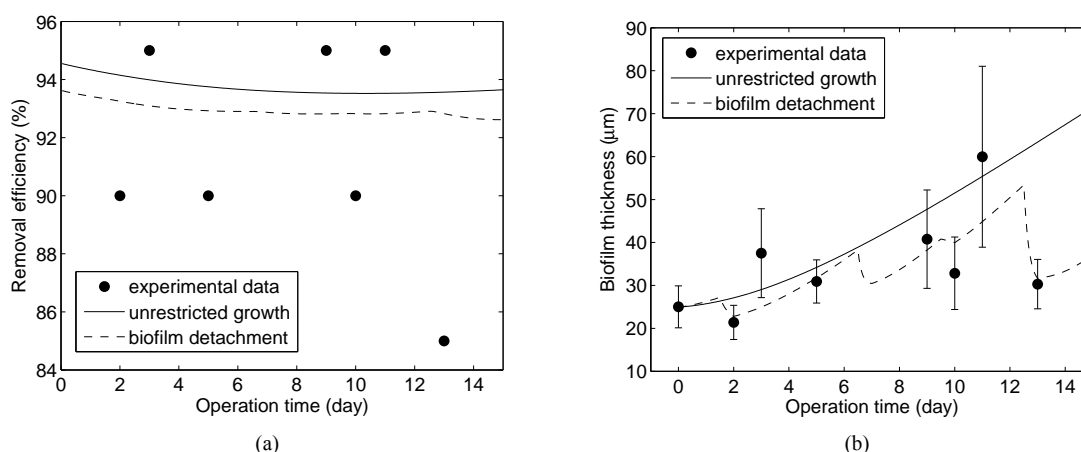


Fig. 6 (a) Comparison of removal efficiencies and (b) the biofilm growth between experimental data (●) and model predictions under the unrestricted growth (solid line) and detachment (dashed line) of biofilm.

ones presented by [6], [7], and [9].

It has been shown that the model, assuming unrestricted growth of microorganisms, accurately predicts the outlet gas concentrations under various operating conditions. When incorporated with sloughing and shear stress, the model is capable of predicting qualitatively the growth of the biofilm and its effect on the removal efficiency. The proposed model should provide useful information on the biofilm growth for the biotrickling filters which are influenced by the variation of the biofilm thickness such as biogas purification process and waste water treatment. Therefore, the model should prove suitable for both system optimization and design in applications.

ACKNOWLEDGMENT

This research project is supported by Thailand Research Fund and Commission on Higher Education, Ministry of Education, Thailand, Faculty of Science and Faculty of Graduate Studies, Mahidol University. The third author is supported by the Center of Excellence in Mathematics, CHE, Thailand.

REFERENCES

- [1] I. V. Ion, F. Popescu, and L. Georgescu, "Mathematical modeling and parameters estimation of an anaerobic digestion of shrimp of culture pond sediment in a biogas process," *International Journal of Energy and Environment*, vol. 1, no. 2, pp. 79–84, 2007.
- [2] D. Kahforoshan, E. Fatehifar, A. A. Babalou, A. R. Ebrahimi, A. Elkamel, and J. S. Soltanmohammadzadeh, "Modeling and evaluation of air pollution from a gaseous flare in an oil and gas processing area," *WSEAS Conferences in Spain, September 2008*, pp. 180–186.
- [3] R. Droste, *Theory and practice of water and wastewater treatment*. New York: John Wiley and Sons, 1997.
- [4] C. Alonso, M. T. Suidan, G. A. Sorial, F. L. Smith, P. Biswas, P. J. Smith, and R. C. Brenner, "Gas treatment in trickle-bed biofilters: biomass, how much is enough?," *Biotechnology and Bioengineering*, vol. 54, no. 6, pp. 583–594, 1997.
- [5] W. J. H. Okkerse, S. P. P. Ottengraf, B. Osinga-Kuipers, and M. Okkerse, "Biomass accumulation and clogging in biotrickling filters for waste gas treatment. evolution of a dynamic model using dichloromethane as a model pollutant," *Biotechnology and Bioengineering*, vol. 63, no. 4, pp. 418–430, 1999.
- [6] S. Kim and M. Deshusses, "Development and experimental validation of a conceptual model for biotrickling filtration of H_2S ," *Environmental Progress*, vol. 22, pp. 119–128, 2003.
- [7] H. Li, J. Crittenden, J. Mihelcic, and H. Hautakangas, "Optimization of biofiltration for odor control: Model development and parameter sensitivity," *Water Environment Research*, vol. 74, pp. 5–16, 2002.
- [8] S. Potvichayanon, *Removal of hydrogen sulfide by fixed-film bioscrubber*. PhD thesis, Mahidol University, Thailand, 2005.
- [9] O. Wanner and W. Gujer, "A multispecies biofilm model," *Biotechnology and Bioengineering*, vol. 28, pp. 314–328, 1986.
- [10] K. Price and R. Storn, "Differential evolution," *Dr. Dobb's Journal*, pp. 18–24, 1997.
- [11] P. Surekha and S. Sumathi, "Solving economic load dispatch problems using differential evolution with opposition based learning," *WSEAS Transactions on Information Science and Applications*, vol. 9, no. 1, pp. 1–13, 2012.
- [12] J. Srisertpol, P. Srinakorn, A. Keawnak, and K. Chamniprasart, "Mathematical modeling and parameters estimation of an anaerobic digestion of shrimp of culture pond sediment in a biogas process," *International Journal of Energy and Environment*, vol. 4, no. 4, pp. 213–220, 2010.
- [13] S. Potvichayanon, P. Pokethitiyook, and M. Krutrachue, "Hydrogen sulfide removal by a novel fixed-film bioscrubber system," *Process Biochemistry*, vol. 41, pp. 708–715, 2006.
- [14] C. J. Mpanias and B. C. Baltzis, "An experimental and modeling study on the removal of mono-chlorobenzene vapor in biotrickling filters," *Biotechnology and Bioengineering*, vol. 59, no. 3, pp. 328–343, 1998.
- [15] R. Perry and D. Green, *Perry's chemical engineers' handbook*. McGraw-Hill, New York, NY, 2008.

- [16] P. Oyarzun, F. Arancibia, C. Canales, and G. E. Aroca, "Biofiltration of high concentration of hydrogen sulphide using," *Process Biochemistry*, vol. 39, pp. 165–170, 2003.
- [17] H. Horn, H. Reiff, and E. Morgenroth, "Simulation of growth and detachment in biofilm systems under defined hydrodynamic conditions," *Biotechnology and Bioengineering*, vol. 81, no. 5, pp. 607–617, 2002.
- [18] G. Baquerizo, J. P. Maestre, T. Sakuma, M. A. Deshusses, X. Gamisans, D. Gabriel, and J. Lafuente, "A detailed model of a biofilter for ammonia removal: model parameters analysis and model validation," *Chemical Engineering Journal*, vol. 113, pp. 205–214, 2005.